Journal of Materials Chemistry C

PAPER

View Article Online
View Journal | View Issue

Cite this: J. Mater. Chem. C, 2017, 5, 12400

Coordination-modulated piezochromism in metal–viologen materials†

Qi Sui,[a] Ye Yuan,[b] Ning-Ning Yang,[a] Xin Li,[b] Teng Gong,[a] En-Qing Gao *[a] and Lin Wang*[b]

Received 14th September 2017,
Accepted 31st October 2017

DOI: 10.1039/c7tc04208f

rsc.li/materials-c

While stimuli-responsive chromic phenomena are well known for various viologen-containing organic and metal–organic materials, viologen-based piezochromism is a very recent discovery in organic compounds. Here we present the first piezochromic metal–viologen material and the modulation of the pressure-responsive behavior through coordination structures. By means of ultraviolet-visible spectroscopy, X-ray photoelectron spectroscopy, electron paramagnetic resonance, *in situ*/*ex situ* X-ray diffraction and DFT calculations, we demonstrated that a zigzag-chain Cd^{II} coordination polymer (**1**) with a viologen-dicarboxylate zwitterionic ligand shows reversible piezochromism, with modulations in threshold pressure and visible-light absorption (color) compared with the free ligand. We also illustrated that piezochromism can be suppressed upon coordination of the same ligand in a rigid 3D framework with the same metal ion. Two basic requirements were proposed from viologen-based piezochromism: appropriate donor–acceptor contacts providing electron transfer pathways, and structural flexibility allowing pressure to further reduce the contacts. We expect great prospects in tuning piezochromism and designing new pressure-responsive materials through diverse metal–viologen combinations. The very fast photochromic response of compound **1** at ambient pressure was also studied, which was attributed to the rather short donor–acceptor contacts in the structure.

Introduction

Chromic materials that change color in response to external stimuli are attractive for applications in many fields such as protection, decoration, optical switching, memory, displays and sensors.[1] Among the most extensively studied chromic materials, compounds containing an electron-deficient viologen (1,1′-disubstituted 4,4′-bipyridinium, also known as paraquat) moiety have been long known for electro-, photo-, and thermochromism owing to the stimulus-induced transformation between the viologen dication and the monocationic radical *via* electron transfer (ET).[2] The viologen moiety has also been widely utilized as a key functional building unit of mechanically interlocked molecules and artificial molecular machines.[3]

Pressure is a fundamental mechanical energy input capable of inducing various changes in physical/chemical properties. In recent years, chromic phenomena induced by pressure (piezochromism)[4] and related mechanical stimuli such as grinding and attrition (tribochromism)[5] have attracted much attention due to their prospective applications such as in pressure sensors and mechano-optical transducers.[1] Piezochromism can also be coupled with luminescence,[4a,6] conductive[7] and magnetic properties[8] to give advanced materials. Very recently, we found that a viologen compound can change color under high pressure,[9] which is the first demonstration of viologen-based piezochromism. Although viologen-based piezo- and photochromism are similar in the sense that both involve ET and consequent radical formation, pressure and light stimuli are very different in the way they affect molecular materials. As is well known, light directly excites individual molecules, and the excited states are quenched by ET in the case of photochromic viologens. Differently, pressure operates in a collective way. It reduces intermolecular distances, and the excess energy arising from intermolecular interactions can be absorbed through intra-/intermolecular structural changes or through bond cleavage/formation.[10] Our work with viologen demonstrated that the energy can be absorbed through ET and radical formation,[9] which represents a new mechanism for organic piezochromism. The discovery of this phenomenon discloses the great potential of the old viologen family to afford novel chromic materials and also has important implications for high-pressure physics and chemistry, which is attracting increasing interest in materials science.[11]

[a] Shanghai Key Laboratory of Green Chemistry and Chemical Processes, School of Chemistry and Molecular Engineering, East China Normal University, 3663 North Zhongshan Road, Shanghai 200062, P. R. China. E-mail: eqgao@chem.ecnu.edu.cn

[b] Center for High Pressure Science and Technology Advanced Research, 1690 Cailun Road, Shanghai 201203, P. R. China. E-mail: wanglin@hpstar.ac.cn

† Electronic supplementary information (ESI) available. CCDC 1526721. For ESI and crystallographic data in CIF or other electronic format see DOI: 10.1039/c7tc04208f

Encouraged by the discovery of viologen-based piezochromism in organic compounds, we extended the study to metal–organic materials. Crystalline metal–organic materials, especially coordination polymers and metal–organic frameworks, have become intriguing platforms for the design of functional materials.[12] With variable compositions and structures, the platforms offer great opportunities to tune the properties arising from different components or from inter-component interplay.[13] In this context, recent years have witnessed a rapid emergence of viologen-containing coordination polymers,[14] of which many are photochromic and some exhibit related properties such as photoswitchable luminescence,[14a] nonlinear optics[14b] and magnetism.[14c,d] Considering that viologen-based piezochromism proceeds through reduction of intermolecular contacts between viologen and electron donors[9] and that metal–organic networks can have different flexibility/rigidity,[15] we suppose that metal coordination could provide a facile handle to control piezochromic behaviors and related properties. Here we present a proof-of-concept. With a flexible one-dimensional (1D) zigzag Cd^{II} coordination polymer (**1**) derived from 4,4′-bipyridinium-1,1′-bis(phenylene-4-carboxylate) (bpybdc), we illustrate the first metal–organic example of piezochromism owing to ET and radical formation. To confirm the possibility of tuning the behavior through metal coordination, the 1D coordination polymer is compared with the piezochromic bpybdc ligand and with a non-piezochromic three-dimensional (3D) coordination polymer derived from the same metal salt and organic ligand. The very fast photochromic response of **1** at ambient pressure is also reported.

Results and discussion

Crystal structure of 1

The mild solvothermal reaction of $Cd(NO_3)_2{\cdot}4H_2O$ and 1,1′-bis(4-carboxylphenyl)-4,4′-bipyridinium dichloride ($[H_2bpybdc]Cl_2$) in a molar ratio of 2 : 1 at 60 °C led to yellow crystals of $[Cd(bpybdc)(NO_3)_2]{\cdot}H_2O$ (**1**). X-ray crystal diffraction analysis revealed that the structure consists of cross-stacked zigzag chains. Each Cd^{II} ion is eight-coordinated in a dodecahedron by four bidentate chelating groups in the *mmmm* arrangement. That is, two nitrate ions and two carboxylate groups span the four *m* edges that define the two perpendicular trapezoids characteristic of a dodecahedron. The combination of the coordination geometry of the metal ion and the linearity of the ligand dictates a zigzag chain (Fig. 1a), with a turn angle (defined by three adjacent metal ions) of 136.861(2)° and a repeat period of 44.059(1) Å. The bpybdc ligand adopts a twisted asymmetric conformation. The two central pyridinium rings are rotated by a dihedral angle of 28.51(28)°, and the two benzene rings form dihedral angles of 46.91(27) and 66.94(31)° with the adjacent pyridinium rings. The conformation is very different from the centrosymmetric conformation (with a strictly planar viologen moiety) observed in the crystalline phase of the free ligand ($bpybdc{\cdot}6H_2O$).[9]

Interchain stacking is worth close inspection due to its importance in intermolecular ET. The zigzag chains are arranged into waved layers along the *bc* plane. The chains in the same layer are parallel and aligned side-by-side, while the chains from neighboring layers propagate along different directions, [041] and [0–41], with a cross angle of 40.3° (Fig. 1b), thus leading to a cross ABAB packing fashion (Fig. 1c). The chains are associated *via* weak C–H···O hydrogen bonds with H···O = 2.38–2.58 Å (Table S1, ESI†). The hydrogen bonds between parallel chains from the same layer involve pyridinium α-/β-H and carboxylate/nitrate O (Fig. 1d), and those between crossing chains from different layers involve benzene H and nitrate O atoms (Fig. S1, ESI†). In addition, there are interchain contacts between pyridinium N atoms and carboxylate/nitrate O atoms (Fig. 1e), which are important for ET in viologen compounds. There are no indications of π–π interactions in the structure.

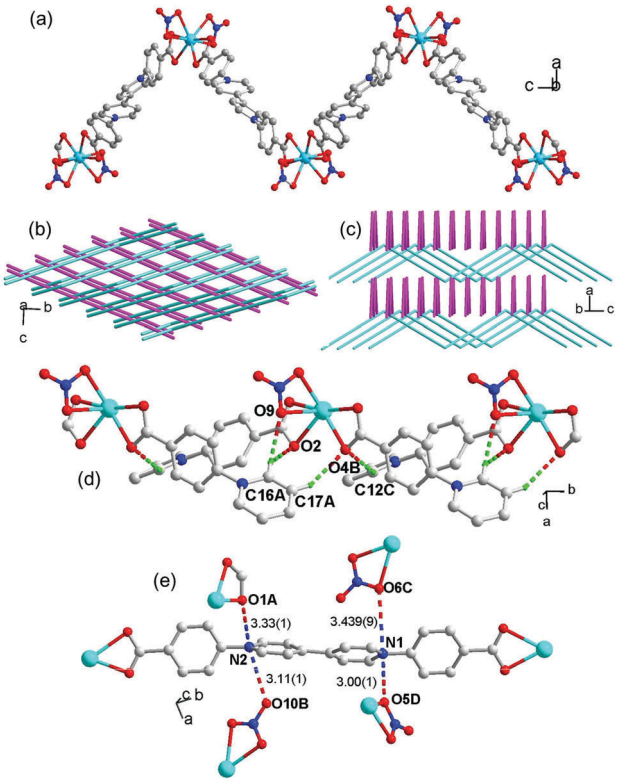

Fig. 1 (a) View of the coordination environment of Cd^{II} in compound **1** (ellipsoids in 50% probability). (b and c) Packing mode of the chains viewed along different directions (different colors); (d) hydrogen bonds between different chains. Symmetry code: *A* = 0.5−*x*, 1 + *y*, 0.5 + *z*; *B* = 0.5−*x*, 2 + *y*, 0.5 + *z*; *C* = *x*, 1 + *y*, *z*; (e) the donor–acceptor contacts in compound **1**. Symmetry code: *A* = 0.5 + *x*, 1−*y*, *z*; *B* = −*x*, 1−*y*, −0.5 + *z*; *C* = 0.5 + *x*, 2−*y*, *z*; *D* = *x*, −1 + *y*, *z*.

Piezochromism

Compound **1** shows a marked color change upon compression. The yellow sample was subjected to anisotropic compression using a hydraulic press for several minutes, and a green solid (**1A**) was obtained after pressure release. Compression in the dark leads to the same color change, precluding the role of light in the process. **1A** gradually turns to yellow again when kept under ambient temperature for several hours either in air or in

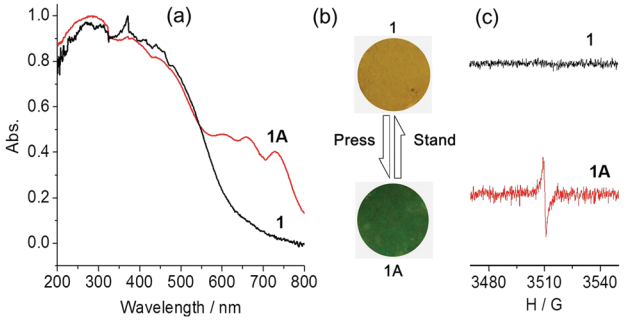

Fig. 2 UV-vis spectra (a) and photographs (b) and EPR spectra (c) of **1** and **1A** (after compression).

nitrogen (Fig. 2b), so the piezochromic process is reversible through spontaneous back electron transfer, as observed for the free bpybdc ligand.[9] The piezochromic phenomenon was confirmed by UV-vis diffuse reflectance spectra (Fig. 2a). The original sample of **1** displays intense absorption bands below 470 nm, with tailing absorption extending to above 600 nm. The absorption band in the visible region is attributed to charge-transfer transitions from the electron-donating carboxylate to the electron-accepting viologen. The green state obtained after compression displays much more strong absorption bands in the visible region, with three obvious maxima at 602, 659 and 731 nm. These maxima are blue-shifted by 8–11 nm compared with the absorption maxima observed for the compression-generated green state of the free bpybdc ligand,[9] reflecting the modulating effect of metal coordination on electronic levels (increasing the energy gaps; the gaps for the lowest-energy bands observed were estimated to be 1.70 and 1.68 eV for the radical states of **1** and the free ligand, respectively, from the band maxima). The effect is visible by the naked eye: the green color of **1A** is more brilliant than the piezo-induced radical state of the ligand. Electron paramagnetic resonance (EPR) spectroscopy was performed to confirm the involvement of radicals in the piezochromic process. As shown in Fig. 2c, **1** is EPR silent, while **1A** presents a single signal with g = 2.0017, which is typical of organic radicals. Powder X-ray diffraction (PXRD) profiles and IR spectra of **1A** show no appreciable changes compared with those of **1** (Fig. S2 and S3, ESI†), suggesting that the crystallographic and molecular structures remain essentially unchanged after the compression–decompression process. This is not surprising because the formation of viologen radicals does not involve bond formation/cleavage but only ET. A few crystallographic reports have revealed that the viologen structure in solids shows minor changes in bond parameters after photochromic radical formation (photo-induced ET).[14f,16] However, it should be noted that, different from photo-induced ET, piezo-induced ET occurs because the high pressure forces closer contacts between electron donors and acceptors.[9] Therefore, the compound actually undergoes some structural changes under high pressure in favor of ET, and the initial structure is recovered upon decompression, although the radicals are retained.

The piezochromic process was further studied by means of pressure-dependent UV-visible spectroscopy using a crystal of **1** in a diamond anvil cell (DAC). The DAC equipment can generate isotropic gigapascal hydrostatic pressure and allows us to monitor the *in situ* changes upon gradual compression and decompression. As shown in Fig. 3a, the crystal shows no obvious absorption in the visible region at the pressure of 0.74 and 2.24 GPa. As the pressure is increased to ~3.5 GPa, the absorption bands at 500, 700 and 780 nm begin to appear, and upon further compression, these bands become more intense and meanwhile show a gradual red shift. The phenomena suggest the gradual formation of radical species upon exertion of pressure. The increasing intensity indicates the increase in the concentration of the radical species, and the red shift could be attributed to the pressured-forced changes in molecular conformation and intermolecular interactions, as generally observed for molecular crystals.[10a,17] Opposite trends were observed during the decompression process (Fig. 3b): the bands show gradual blue-shifts and decreasing intensity, indicating the gradual quenching of radicals through back ET. There is obvious hysteresis in the decompression process, as clearly shown in Fig. 3c. Even after complete release of pressure, the radical still remains in a certain amount. The absorption maxima of the resulting green crystal are at the same wavelengths as those for the green powder obtained by compression and decompression using a hydraulic press (Fig. 2a), indicating that the piezochromism of **1** proceeds through the same radical mechanism either under the isotropic pressure of DAC or under the anisotropic pressure of a hydraulic press. According to the studies with DACs, the crystals of coordination polymer **1** and the free ligand show at least two different

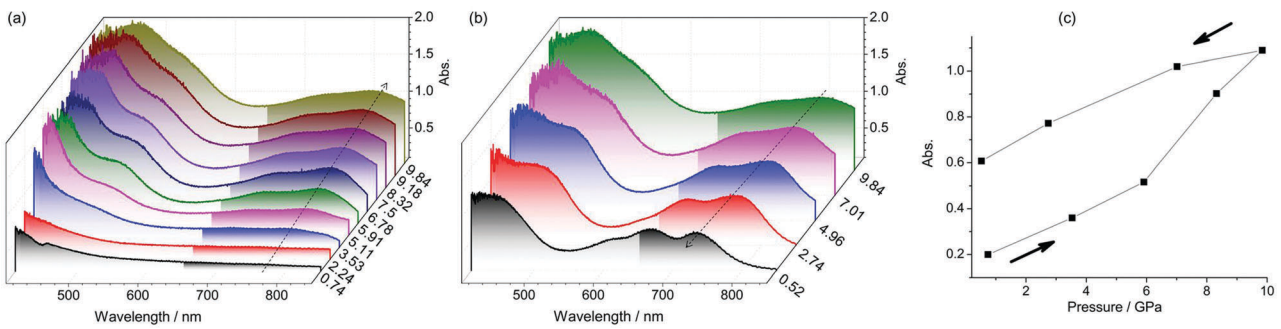

Fig. 3 Pressure-dependent UV-vis spectra of compound **1** during compression (a) and decompression (b) in a DAC. (c) The variation of the maximum absorbance of **1** around 800 nm during compression and decompression.

features in their piezochromic behaviors. First, the coordination polymer needs higher pressure to initiate the piezochromic process. The radical begins to form in the pure organic phase at about 2 GPa, as indicated by the appearance of new absorption bands in the 600–800 nm region and the observation of a weak but visible color change under an optical microscope. The coordination polymer does not show an appreciable color change and absorption bands indicative of radical formation. Second, the free ligand turns red gradually upon compression and does not become green until decompression below 2 GPa, where the red color is because the absorption bands under high pressure are stronger below 600 nm than above that wavelength. Differently, for **1**, green is the main hue under high pressure and after decompression, which is consistent with the higher absorption above 650 nm than that around 600 nm. The results illustrate that metal coordination can at least have modulating effects on the threshold pressure and the high-pressure color.

X-ray photoelectron spectroscopy (XPS) was performed to provide evidence for the direction of ET. As shown in Fig. 4, the Cd 3d core-level bands are almost the same before and after compression, consistent with the inertness of Cd^{II} to ET. The N 1s bands of **1** are close to the Cd $3d_{5/2}$ peak. The band at 402.1 eV could be attributed to N in the pyridinium ring,[18] while the signal of the nitrate N atom is at 406.4 eV.[19] The latter is submerged in the Cd $3d_{5/2}$ band, as confirmed by multi-peak resolution (Fig. S4, ESI†). After compression, **1A** shows an additional weak N 1s signal at lower energy around 400.0 eV, which could indicate the formation of viologen radicals. The C 1s spectrum of **1** shows three peaks. The carboxylate group is responsible for the weakest peak at 288.0 eV, while the main peak at 284.8 eV and the shoulder at about 286.1 eV arise from phenylene and pyridinium groups.[19] After compression, the carboxylate band is broadened towards higher energy, and meanwhile the intensity of the shoulder is decreased relative to the main peak. These phenomena support the assumption that carboxylate and pyridinium serve as electron donors and acceptors, respectively. The O 1s spectrum of **1** appears as an asymmetric broad envelope in the range from 529 to 535 eV, owing to the contributions mainly from carboxylate and nitrate. After compression, the relative intensity of the low-energy shoulder decreases, suggesting that some of the O atoms serve as electron donors.[20]

Photochromism

Compound **1** also shows photochromism at ambient pressure, in contrast with the free ligand, which is piezochromic but not photochromic.[9] When irradiated with a xenon lamp (300 W), the crystals of **1** turn from yellow to green (Fig. 5a). The photochromic phenomenon is also observed under sunlight (Fig. S5, ESI†). The green state (denoted as **1B**) recovers to the initial yellow state when standing in the dark for hours. The color recovery can be accelerated by heating. The photo-switched color change can be repeated (Fig. S6, ESI†). The PXRD profile and the IR spectrum (Fig. S7 and S8, ESI†) of **1B** are identical to those of **1**, suggesting that there are no significant differences in crystallographic or molecular structures between the two states. The EPR spectrum of **1B** shows a radical signal, similar to the case of **1A** (Fig. S9, ESI†), so the photochromism from **1** to **1B** is also due to the formation of radicals through ET.

Moreover, it is notable that the compound is very fast in its response to light. An obvious color change can be observed by the naked eye immediately upon irridiation (within 1 s), and the coloration saturates to a photostationary state within about 30 s, as shown in Fig. 5b. The kinetics of the photochromic reaction was analyzed using the kinetic equation $\ln((A_0 - A)/(A_t - A)) = kt$, where k is the first-order rate constant and A_0, A_t and A are the absorbance bands at 726 nm at the beginning, at irridiation time t and in the photostationary state, respectively.[21] The linear fit of the data (Fig. 5c and d) indicates that the photoinduced

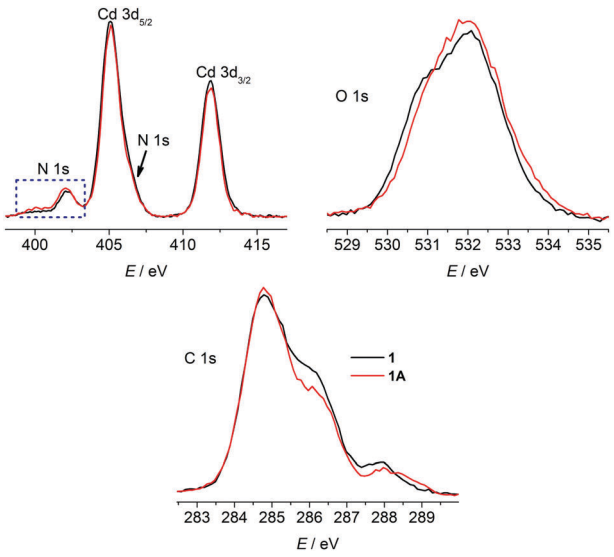

Fig. 4 XPS spectra of **1** (black) and **1A** (red, compressed).

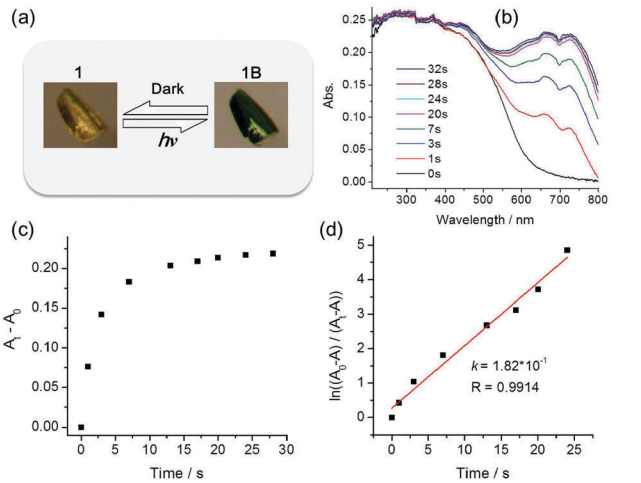

Fig. 5 Photographs (a) of **1** before and after irradiation by Xe light and UV-vis spectra at different irradiation times (b); solid state kinetic traces: (c and d) photoinduced electron-transfer process based on UV-vis absorption at 726 nm.

ET process follows the first-order reaction kinetics, with the rate constant being $k = 0.182\ s^{-1}$. Notably, the value of k is a hundred times larger than those for analogue compounds with viologen derived ligands.[22]

Considering that the pristine yellow state of **1** and the pressure- and photogenerated green states (**1A** and **1B**) show essentially identical PXRD and IR profiles (Fig. S2, S3, S7 and S8, ESI†), they may be classified as special types of isomorphs that show no significant differences in crystallographic or molecular structures but differ from one another in electronic structure or radical content. The pristine state is radical-free, while **1A** and **1B** contain different concentrations of radicals as indicated by the different intensities in ESR and visible-light spectra.

Further insight into the chromic phenomena

It is worthwhile to check the structure for the pathways of ET. A possible pathway generally assigned for photochromic viologen compounds is the short intermolecular contact (3–4 Å) between the pyridinium N atom and the donor atom that approaches the N atom from either side of the pyridinium plane.[23] As shown in Fig. 1e, **1** possesses short interchain $O_{carboxylate/nitrate}\cdots N_{pyridinium}$ contacts in the range of 3.00(1)–3.439(9) Å, which are appropriate for photo-induced ET. Another possible pathway is the hydrogen bonding contacts between C–H groups α to the pyridinium N atom and the donor atoms.[24] Such contacts also exist between the zigzag chains in **1**, with the $\alpha\text{-}H_{pyridinium}\cdots O_{carboxylate/nitrate}$ distances being 2.38–2.46 Å (Fig. 1d). The above data indicate that both carboxylate and nitrate can serve as electron donors.

The total and partial density of states (DOS) were calculated using the crystallographic data of **1** to gain more insight into the ET. As shown in Fig. 6, the first two DOS bands below the Fermi level are overwhelmingly dominated by the nitrate and carboxylate groups, while the low-energy bands above the Fermi level are mainly contributed by the pyridinium group. The results support that ET occurs from nitrate and/or carboxylate to pyridinium, consistent with the experimental XPS analysis. Further DFT calculations were performed using the DMol^3 module for the binuclear model molecule $Cd_2(bpybdc)(NO_3)_4$ (Fig. 7b) in the closed-shell singlet (spin-restricted) and open-shell triplet (spin-unrestricted) states. Molecular orbitals were calculated after geometry optimization. As shown in Fig. 7a, the lowest unoccupied molecular orbital (LUMO) of the binuclear molecule in the singlet state is predominantly composed of a viologen-based π orbital, and the highest occupied molecular orbitals (HOMOs) mainly arise from the nitrate O atoms, with HOMO−1 possessing some contribution from the carboxylate O atoms. Therefore, under appropriate stimuli, ET from nitrate and carboxylate to viologen can occur, provided that there are appropriate pathways. The calculations with the triplet state indeed indicated that one spin-unpaired electron is distributed over the viologen group and the other one is delocalized over the nitrate/carboxylate groups, according to the different occupations of the orbitals for α and β spin (Fig. 7a). Fig. 7c also clearly illustrates that the spin densities are overwhelmingly distributed over the viologen, nitrate and carboxylate moieties.

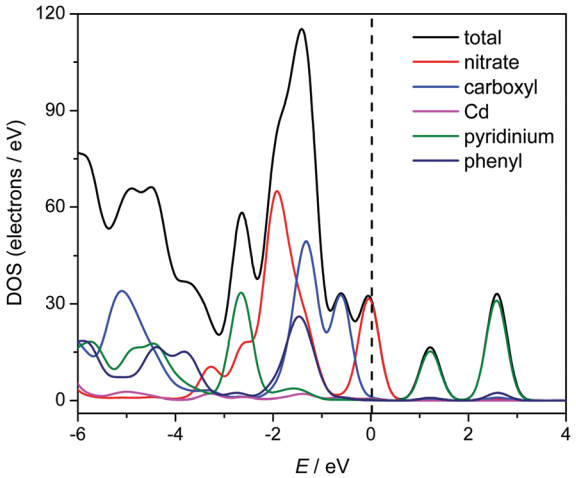

Fig. 6 Total and partial density of states calculated from the single-crystal data of **1**. The Fermi level is located at 0 eV (dashed line).

The fast photochromic response of **1** could be due to the rather short $O\cdots N_{pyridinium}$ donor–acceptor contacts (3.00(1)–3.439(9) Å) in the structure, which facilitate fast ET upon absorption of light energy. For comparison, the distances in the non-photochromic crystal of the free bpybdc ligand (bpybdc·$6H_2O$) are all above 3.5 Å.[9] While light energy can be directly absorbed by molecules in solids through electronic transitions, pressure, as a kind of mechanical energy input, interacts with molecular solids in quite different ways. Covalent bonds are usually rather resistant to pressure,[25] but a molecular crystal can respond to high pressure through reduction of the intermolecular space and through changes of molecular conformation. For the piezochromism of the crystal of the free bpybdc ligand, it has been proposed that high pressure serves to force closer intermolecular donor–acceptor contacts so as to induce ET without the aid of light. Analogously, the interchain distance in **1** can be reduced by pressure, and the conformation of the zigzag chain could also be adjustable through changes in the metal coordination sphere and in the conformation of the bpybdc ligand. The inter- and intrachain changes forced by pressure could work in synergy to reduce the donor–acceptor contacts and thereby to induce ET. It should be noted that the viologen moiety in **1** is nonplanar, with a twist angle of 28.51(28)° between the two pyridinium rings. Since the viologen radical prefers the planar conformation, the formation of the radical from a twisted viologen precursor should need more energy than from a planar precursor. This could explain the higher threshold pressure for **1** compared with the free ligand, where the viologen moiety is planar.

The above results suggest that the piezochromic properties of the bpybdc ligand can be inherited by its coordination polymers, with some modulations in onset pressure and in color owing to variations in the molecular and electronic structures after coordination. We expect that there are great opportunities for tuning piezochromism through coordination chemistry, especially through the versatile platforms of coordination polymers. With this in mind, we synthesized a 3D coordination polymer (**2**) with the same metal center and organic ligand as those in **1**.

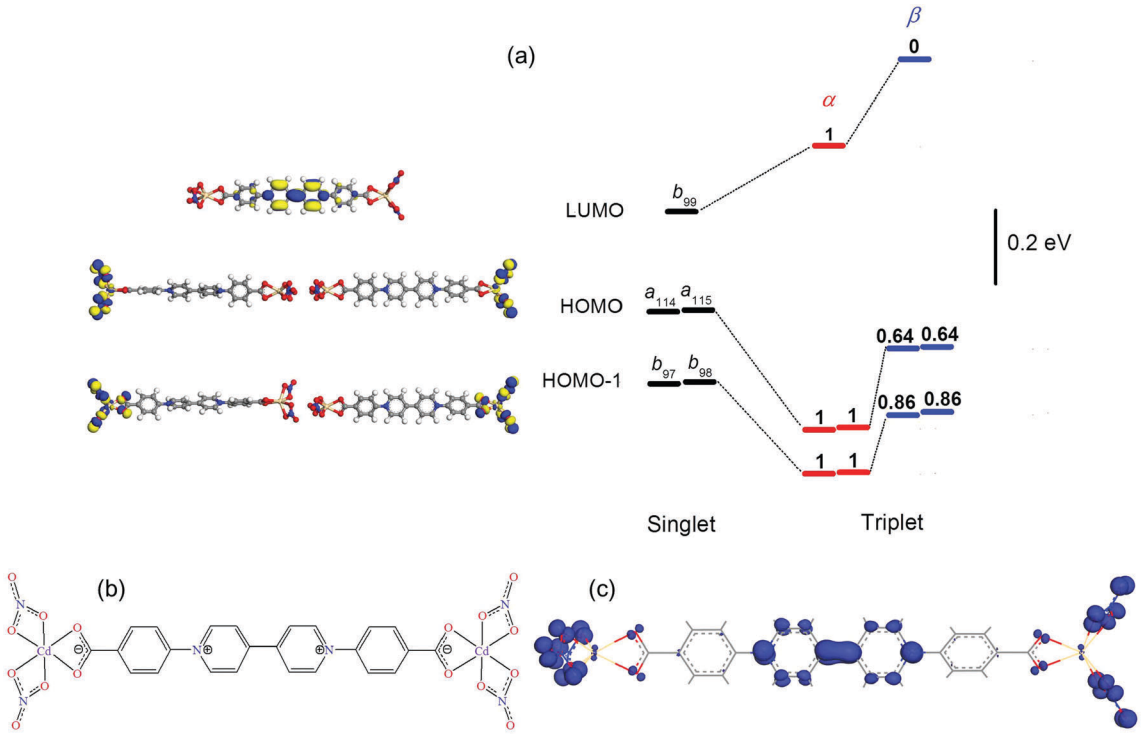

Fig. 7 (a) Calculated frontier molecular orbital profiles for the model complex $[Cd_2(bpybdc)(NO_3)_4]$. The orbitals are labelled by a and b (irreducible representations of the C_2 point group) with the orbital numbers as subscripts. The numbers above the orbitals of the triplet state are the electron occupation of the orbitals. (b) A schematic presentation of the model complex. (c) The spin density distribution for the triplet state.

The crystal structure of **2** has been recently determined, which shows a rigid 3D framework in which D_3-symmetric $[Cd\{(\mu\text{-}Cl)_2Cd(CO_2)_2\}_3]$ clusters are linked by the backbones of the bpybdc ligands, with $[CdCl_4]^{2-}$ counter-anions enclosed in channels.[26] There are also short electron donor–acceptor contacts in **2**, with the $O_{carboxylate}\cdots N_{pyridinium}$ and $Cl\cdots N_{pyridinium}$ distances being 3.579(8) and 3.408(8) Å, respectively. The contacts are comparable to those in **1** and in the crystal of the free ligand, but we did not see any indication of piezochromism for **2** under the conditions applied for **1** and the ligand. It is reasonable to assume that the rigid 3D framework of **2** is less compressible than the structures built of 1D $[Cd(bpybdc)]_n$ chains or "0D" bpybdc molecules. The donor–acceptor contacts in the 3D framework are rather insensitive to the applied pressure and cannot be pushed close enough to evoke ET, so no piezochromism occurs. Compound **2** illustrates the extreme case of coordination modulation, where the rigidity of the 3D framework suppresses piezochromism by preventing the donors and acceptors from approaching each other close enough for ET. According to these results, two basic ingredients are required for piezochromism in viologen-derived materials: there should be appropriate electron donors in close proximity to viologen moieties, and the structure should be flexible enough for pressure to push the donors and acceptors even closer.

To prove the above conjecture, we performed DFT geometry optimization for compound **1** under pressure using the CASTEP module and investigated the effects of pressure on the crystal structure and donor–acceptor contacts. The lattice parameters and selected structural data for the X-ray crystallographic structure (the initial model) and for the optimized structures under the hydrostatic pressures of 0 and 3.5 GPa are listed in Table S2 (ESI†). Compared with the optimized zero-pressure structure, which is in good agreement with the crystallographic results, the structure optimized under 3.5 GPa shows changes in both intrachain and interchain parameters. The important changes within the zigzag chain including the changes (−4.3–0.4°) of the dihedral angles in the organic ligand, the shortening (by 0.24 Å) of the Cd···Cd distance spanned by the ligand and the expansion (by 2.9°) of the Cd···Cd···Cd turn angle. The compensation between the last two changes leads to a negligible reduction in the repeat period of the chain. As expected, the changes in the interchain parameter are more significant. The interchain distances within the layer of parallel chains are reduced from 3.62 to 3.22 Å, and the interlayer distances change from 7.78 to 7.28 Å. The acute angle between the two different propagation directions of chains is reduced from 41.1 to 35.8°. These structural changes are reflected by a moderate contraction, a minor expansion, and a significant contraction along the *a*, *b* and *c* axes of the unit cell, respectively, with an overall contraction of 16.9% (420.4 $Å^3$) in the cell volume. Most relevant to piezochromism are the changes of interchain donor–acceptor contacts in response to compression. As can be seen from Fig. S10 (ESI†), the N···O distances between viologen and carboxylate/nitrate moieties are significantly reduced from 2.94–3.34 Å at zero pressure to 2.68–2.87 Å under 3.5 GPa. The $\alpha\text{-}H_{pyridinium}\cdots O$ distances are also significantly

shortened from 2.24–2.40 to 1.96–2.25 Å (Table S2, ESI†). The results support that the flexibility of the chain-based structure of **1** allows significant reduction in donor–acceptor contacts under high pressure, to benefit spontaneous ET without the aid of other stimuli. For comparison, geometry optimization under high pressure was also performed on the 3D framework of **2**. The results (Table S3, ESI†) suggest that the structure under 3.5 GPa undergoes a less significant reduction (by 5.0%) in volume, which is mainly related to the contraction along the *c* direction (the 3-fold axis of the structure). Most importantly, although reduced to some degree under the pressure, the $O_{carboxylate}\cdots N_{pyridinium}$ and $Cl\cdots N_{pyridinium}$ distances under 3.5 GPa are still larger than 3.3 Å, which might not be close enough for spontaneous ET. Therefore, compared with the chain-based structure of **1**, the 3D framework of **2** is less compressible, and the donor–acceptor distances are not so sensitive to high pressure, which prevents piezochromism.

Conclusions

We have revealed that the 1D zigzag Cd^{II} coordination polymer **1** with the viologen-dicarboxylate zwitterionic ligand bypbdc shows reversible piezochromism. The compound also shows photochromism with a very fast response rate owing to the rather short donor–acceptor contacts. The chromic phenomena are attributed to the formation of radicals through ET from nitrate/carboxylate to the viologen moiety. While ET photochromism has been widely demonstrated, this work is the first demonstration of ET piezochromism in metal–organic materials. The hybrid compound does not simply reproduce the ligand-based piezoresponsive behavior. Instead, the coordination structure has significant impacts on piezosensitivity. The flexible chain-based structure of **1** leads to modulations in threshold pressure and high-pressure color (light absorption), while a rigid 3D metal–organic framework can even suppress the piezoresponsive behavior. Two basic structural requirements were proposed for viologen-based piezochromism: appropriate donor–acceptor contacts providing ET pathways, and structural flexibility allowing pressure to promote further closer contacts for ET. The study of ET piezochromism is still at the beginning, but we believe that our results can open new prospects for the design of pressure-responsive materials. The remarkable diversity in coordination bonds and networks can provide great opportunities to alter the donor–acceptor contacts and structural flexibility, so we expect that coordination chemistry (especially the formation of coordination polymers) can be a versatile tool to tune piezochromic properties. The tool is also very appealing for the potential of combining viologen-based piezochromism and the properties arising from metal chromophores (such as magnetism and luminescence).

Experimental section

Physical measurements and computations are described in the ESI.†

Materials and synthesis

4,4′-bipy, 2,4′-dinitrochlorobenzene, ethyl *p*-aminobenzoate and NaOH in AR grade were purchased commercially without further purification. Water was deionized and distilled before use. The ligand $[H_2bpybdc]Cl_2$ was prepared according to our previous work.[9] A mixture of ligand (0.02 mmol, 0.010 g), $Cd(NO_3)_2\ 4H_2O$ (0.04 mmol, 0.013 g), DMF (2 ml) and MeOH (1 ml) was stirred for 15 min, then sealed in a 20 ml vial and kept at 60 °C for 12 h. The yellow crystals of compound **1** were obtained after slowly cooling to room temperature (42% yield based on ligand). Its phase purity was checked by PXRD (Fig. S2, ESI†) and the IR spectrum is shown in Fig. S3 (ESI†). Elemental analysis calc. for $C_{24}H_{20}N_4O_{11}Cd$, (M = 652.84): C, 44.15; H, 3.09; N, 8.58; found: C, 43.98; H, 3.14; N, 8.21%.

Crystal structure determination

Diffraction intensity data of **1** were collected using graphite-monochromated Mo-Kα radiation (0.71073 Å) at 293 K on a Bruker APEX II diffractometer equipped with a CCD area detector. Empirical absorption corrections were applied using the SADAB program.[27] The structures were solved using the direct method and refined using the full-matrix least-squares method on F^2 using the SHELXL program,[28] with anisotropic displacement parameters for all non-hydrogen atoms. The hydrogen atoms attached to carbon atoms were placed in calculated positions and refined using the riding model. The water hydrogen atoms were located from the difference Fourier map.

Crystal data for **1**: $C_{24}H_{20}N_4O_{11}Cd$, M_r = 652.84, space group $Pca2_1$, a = 15.6931(4), b = 10.3418(3), c = 15.1640(4), T = 173(2) K, Z = 4, V = 2461.04(12) Å^3, D_c = 1.762 g cm^{-3}, μ = 7.754 mm^{-1}, $F(000)$ = 1312 and GOF = 1.094. 26716 reflections collected, 4473 unique (R_{int} = 0.0254). R_1 = 0.0362, wR_2 = 0.1048 [$I > 2\sigma(I)$]. CCDC 1526721.†

Conflicts of interest

There are no conflicts to declare.

Acknowledgements

This work was supported by the National Natural Science Foundation of China (Grant No. 21471057 and 21773070). Y. Y., X. L., and L. W. would like to acknowledge the support of NSAF (Grant No. U1530402) and Science Challenging Program (Grant No. JCKY2016212A501).

Notes and references

1 P. Bamfield and M. G. Hutchings, *Chromicm Phenomena: Technological Applications of Colour Chemistry*, RSC, Cambridge, 2nd edn, 2010.
2 P. M. S. Monk, *The Viologens. Physicochemical properties, synthesis and applications of the salts of 4,4′-bipyridine*, Wiley-VCH Verlag GmbH, 1999.

3 (*a*) P. R. McGonigal, P. Deria, I. Hod, P. Z. Moghadam, A.-J. Avestro, N. E. Horwitz, I. C. Gibbs-Hall, A. K. Blackburn, D. Chen, Y. Y. Botros, M. R. Wasielewski, R. Q. Snurr, J. T. Hupp, O. K. Farha and J. F. Stoddart, *Proc. Natl. Acad. Sci. U. S. A.*, 2015, **112**, 11161–11168; (*b*) S. Erbas-Cakmak, D. A. Leigh, C. T. McTernan and A. L. Nussbaumer, *Chem. Rev.*, 2015, **115**, 10081–10206; (*c*) C. Cheng, P. R. McGonigal, S. T. Schneebeli, H. Li, N. A. Vermeulen, C. Ke and J. F. Stoddart, *Nat. Nanotechnol.*, 2015, **10**, 547–553.

4 (*a*) K. Nagura, S. Saito, H. Yusa, H. Yamawaki, H. Fujihisa, H. Sato, Y. Shimoikeda and S. Yamaguchi, *J. Am. Chem. Soc.*, 2013, **135**, 10322–10325; (*b*) Y. Dong, B. Xu, J. Zhang, X. Tan, L. Wang, J. Chen, H. Lv, S. Wen, B. Li, L. Ye, B. Zou and W. Tian, *Angew. Chem., Int. Ed.*, 2012, **51**, 10782–10785.

5 (*a*) Piezochromism and tribochromism are two subclasses of mechanochromism (ref. 1). The two chromic phenomena do not necessarily coexist or share the same color and mechanism because the grinding and attrition stimuli for tribochromism can cause various effects other than compression. Moreover, they have very different implications for applications. In the literature, however, grinding-induced color change has sometimes been confusingly called ''piezochromism''. There is a need to clearly discriminate between them as such materials are increasing rapidly; (*b*) J.-K. Sun, C. Chen, L.-X. Cai, C.-X. Ren, B. Tan and J. Zhang, *Chem. Commun.*, 2014, **50**, 15956–15959; (*c*) Z.-L. Zhang, D.-D. Yao, T.-L. Zhou, H.-Y. Zhang and Y. Wang, *Chem. Commun.*, 2011, **47**, 7782–7784; (*d*) Z. H. Guo, Z. X. Jin, J. Y. Wang and J. Pei, *Chem. Commun.*, 2014, **50**, 6088–6090.

6 Q. Qi, J. Qian, X. Tan, J. Zhang, L. Wang, B. Xu, B. Zou and W. Tian, *Adv. Funct. Mater.*, 2015, **25**, 4005–4010.

7 A. Jaffe, Y. Lin, W. L. Mao and H. I. Karunadasa, *J. Am. Chem. Soc.*, 2015, **137**, 1673–1678.

8 D. Pinkowicz, M. Rams, M. Misek, K. V. Kamenev, H. Tomkowiak, A. Katrusiak and B. Sieklucka, *J. Am. Chem. Soc.*, 2015, **137**, 8795–8802.

9 Q. Sui, X. T. Ren, Y. X. Dai, K. Wang, W. T. Li, T. Gong, J. J. Fang, B. Zou, E. Q. Gao and L. Wang, *Chem. Sci.*, 2017, **8**, 2758–2768.

10 (*a*) Y. Wang, X. Tan, Y. M. Zhang, S. Zhu, I. Zhang, B. Yu, K. Wang, B. Yang, M. Li, B. Zou and S. X. A. Zhang, *J. Am. Chem. Soc.*, 2015, **137**, 931–939; (*b*) K. Lekin, H. Phan, S. M. Winter, J. W. L. Wong, A. A. Leitch, D. Laniel, W. Yong, R. A. Secco, J. S. Tse, S. Desgreniers, P. A. Dube, M. Shatruk and R. T. Oakley, *J. Am. Chem. Soc.*, 2014, **136**, 8050–8062; (*c*) J. W. Wong, A. Mailman, K. Lekin, S. M. Winter, W. Yong, J. Zhao, S. V. Garimella, J. S. Tse, R. A. Secco, S. Desgreniers, Y. Ohishi, F. Borondics and R. T. Oakley, *J. Am. Chem. Soc.*, 2014, **136**, 1070–1081; (*d*) Y. Tian, K. Uchida, H. Kurata, Y. Hirao, T. Nishiuchi and T. Kubo, *J. Am. Chem. Soc.*, 2014, **136**, 12784–12793; (*e*) M. Souto, H. Cui, M. Pena-Alvarez, V. G. Baonza, H. O. Jeschke, M. Tomic, R. Valenti, D. Blasi, I. Ratera, C. Rovira and J. Veciana, *J. Am. Chem. Soc.*, 2016, **138**, 11517–11525; (*f*) I. F. Bruce-Smith, B. A. Zakharov, J. Stare, E. V. Boldyreva and C. R. Pulham, *J. Phys. Chem. C*, 2014, **118**, 24705–24713.

11 L. Zhang, Y. Wang, J. Lv and Y. Ma, *Nat. Rev. Mater.*, 2017, **2**, 17005.

12 (*a*) X. Cao, C. Tan, M. Sindoro and H. Zhang, *Chem. Soc. Rev.*, 2017, **46**, 2660–2677; (*b*) N. S. Bobbitt, M. L. Mendonca, A. J. Howarth, T. Islamoglu, J. T. Hupp, O. K. Farha and R. Q. Snurr, *Chem. Soc. Rev.*, 2017, **46**, 3357–3385; (*c*) M. Bosch, S. Yuan, W. Rutledge and H.-C. Zhou, *Acc. Chem. Res.*, 2017, **50**, 857–865.

13 (*a*) R.-W. Huang, Y.-S. Wei, X.-Y. Dong, X.-H. Wu, C.-X. Du, S.-Q. Zang and T. C. W. Mak, *Nat. Chem.*, 2017, **9**, 689–697; (*b*) C. Sun, M.-S. Wang, P.-X. Li and G.-C. Guo, *Angew. Chem., Int. Ed.*, 2017, **56**, 554–558; (*c*) N. Sikdar, K. Jayaramulu, V. Kiran, K. V. Rao, S. Sampath, S. J. George and T. K. Maji, *Chem. – Eur. J.*, 2015, **21**, 11701–11706; (*d*) R. X. Yao, X. Cui, X. X. Jia, F. Q. Zhang and X. M. Zhang, *Inorg. Chem.*, 2016, **55**, 9270–9275; (*e*) S. Rodriguez-Jimenez, H. L. Feltham and S. Brooker, *Angew. Chem., Int. Ed.*, 2016, **55**, 15067–15071.

14 (*a*) J. Wang, S. L. Li and X. M. Zhang, *ACS Appl. Mater. Interfaces*, 2016, **8**, 24862–24869; (*b*) H.-Y. Li, H. Xu, S.-Q. Zang and T. C. W. Mak, *Chem. Commun.*, 2016, **52**, 525–528; (*c*) T. Gong, X. Yang, J.-J. Fang, Q. Sui, F.-G. Xi and E.-Q. Gao, *ACS Appl. Mater. Interfaces*, 2017, **9**, 5503–5512; (*d*) T. Gong, X. Yang, Q. Sui, Y. Qi, F. G. Xi and E. Q. Gao, *Inorg. Chem.*, 2016, **55**, 96–103; (*e*) H. Y. Li, Y. L. Wei, X. Y. Dong, S. Q. Zang and T. C. W. Mak, *Chem. Mater.*, 2015, **27**, 1327–1331; (*f*) W. Shi, F. Xing, Y. L. Bai, M. Hu, Y. Zhao, M. X. Li and S. Zhu, *ACS Appl. Mater. Interfaces*, 2015, **7**, 14493–14500; (*g*) N.-N. Yang, W. Sun, F.-G. Xi, Q. Sui, L.-J. Chen and E.-Q. Gao, *Chem. Commun.*, 2017, **53**, 1747–1750; (*h*) M. S. Wang, G. Xu, Z. J. Zhang and G. C. Guo, *Chem. Commun.*, 2010, **46**, 361–376.

15 A. Schneemann, V. Bon, I. Schwedler, I. Senkovska, S. Kaskel and R. A. Fischer, *Chem. Soc. Rev.*, 2014, **43**, 6062–6096.

16 (*a*) G. Xu, G. C. Guo, M. S. Wang, Z. J. Zhang, W. T. Chen and J. S. Huang, *Angew. Chem., Int. Ed.*, 2007, **46**, 3249–3251; (*b*) G. Xu, G.-C. Guo, J.-S. Guo, S.-P. Guo, X.-M. Jiang, C. Yang, M.-S. Wang and Z.-J. Zhang, *Dalton Trans.*, 2010, **39**, 8688–8692.

17 X. Meng, G. Qi, C. Zhang, K. Wang, B. Zou and Y. Ma, *Chem. Commun.*, 2015, **51**, 9320–9323.

18 (*a*) Y.-N. Gong and T.-B. Lu, *Chem. Commun.*, 2013, **49**, 7711–7713; (*b*) X.-Y. Lv, M.-S. Wang, C. Yang, G.-E. Wang, S.-H. Wang, R.-G. Lin and G.-C. Guo, *Inorg. Chem.*, 2012, **51**, 4015–4019; (*c*) M. S. Wang, C. Yang, G. E. Wang, G. Xu, X. Y. Lv, Z. N. Xu, R. G. Lin, L. Z. Cai and G. C. Guo, *Angew. Chem., Int. Ed.*, 2012, **51**, 3432–3435.

19 V. I. Nefedov, *X-ray Photoelectron Spectroscopy of Chemical Compounds: Handbook*, Khimiya, 1984.

20 (*a*) Z. J. Zhang, S. C. Xiang, G. C. Guo, G. Xu, M. S. Wang, J. P. Zou, S. P. Guo and J. S. Huang, *Angew. Chem., Int. Ed.*, 2008, **47**, 4149–4152; (*b*) J. T. Sampanthar, K. G. Neoh, S. W. Ng, E. T. Kang and K. L. Tan, *Adv. Mater.*, 2000, **12**, 1536–1539.

21 J. Sworakowski, K. Janus and S. Nespurek, *Adv. Colloid Interface Sci.*, 2005, **116**, 97–110.

22 (*a*) Y. Zeng, S. Liao, J. Dai and Z. Fu, *Chem. Commun.*, 2012, **48**, 11641–11643; (*b*) M. Fan, Z. Yao, C. Li, Y. Xia, Q. Zhang,

J. Dai and Z. Fu, *CrystEngComm*, 2013, **15**, 8408–8411; (*c*) R. G. Lin, G. Xu, G. Lu, M. S. Wang, P. X. Li and G. C. Guo, *Inorg. Chem.*, 2014, **53**, 5538–5545; (*d*) R. G. Lin, G. Xu, M. S. Wang, G. Lu, P. X. Li and G. C. Guo, *Inorg. Chem.*, 2013, **52**, 1199–1205.

23 (*a*) J.-K. Sun, L.-X. Cai, Y.-J. Chen, Z.-H. Li and J. Zhang, *Chem. Commun.*, 2011, **47**, 6870–6872; (*b*) D. Aulakh, A. P. Nicoletta, J. R. Varghese and M. Wriedt, *CrystEngComm*, 2016, **18**, 2189–2202; (*c*) J. K. Sun, P. Wang, Q. X. Yao, Y. J. Chen, Z. H. Li, Y. F. Zhang, L. M. Wu and J. Zhang, *J. Mater. Chem.*, 2012, **22**, 12212–12219.

24 (*a*) W.-B. Li, Q. Yao, L. Sun, X.-D. Yang, R.-Y. Guo and J. Zhang, *CrystEngComm*, 2016, **19**, 722–726; (*b*) O. Toma, N. Mercier, M. Allain, A. A. Kassiba, J.-P. Bellat, G. Weber and I. Bezverkhyy, *Inorg. Chem.*, 2015, **54**, 8923–8930.

25 (*a*) L. Wang, K. Wang, B. Zou, K. Ye, H. Zhang and Y. Wang, *Adv. Mater.*, 2015, **27**, 2918–2922; (*b*) W. Cai, J. He, W. Li and A. Katrusiak, *J. Mater. Chem. C*, 2014, **2**, 6471–6476.

26 M. Leroux, N. Mercier, M. Allain, M. C. Dul, J. Dittmer, A. H. Kassiba, J. P. Bellat, G. Weber and I. Bezverkhyy, *Inorg. Chem.*, 2016, **55**, 8587–8594.

27 G. M. Sheldrick, *SADABS, Program for Empirical Absorption Correction*, University of Göttingen, Göttingen, Germany, 1996.

28 G. M. Sheldrick, *SHELXTL. Bruker Analytical X-ray Instruments Inc.*, Madison, Wisconsin, USA, 1998.

